

CrossRef DOI of original article:

1 Topology Optimization: Applications of VFLSM and SESO in 2 the Generation of Three-Dimensional Strut-and-Tie Models

3 Vitor Manuel A. Leitão

4 *Received: 1 January 1970 Accepted: 1 January 1970 Published: 1 January 1970*

6 Abstract

7 This article presents the analysis of Strut-and-Tie Model (STM) in reinforced concrete 3D
8 structures based on the study of topological optimization, so that the problem is formulated
9 with the Smooth-ESO (SESO) discrete method, whose removal heuristic is bidirectional with
10 discrete optimization procedure, and the Velocity Field Level Set Method (VFLSM), which is
11 an inheritance of the classical continuum Level Set Method (LSM), but advances the design
12 limits with a velocity field constructed from the rate of the design variables and base
13 functions. The proposed approach is to couple both methods in conjunction with the Method
14 of Moving Asymptotes (MMA), used to control the various design constraints that are the
15 minimization of compliance and the Von Mises stress that has demonstrated more rational
16 STM results. Additionally, it has been formulated a methodology for the automatic generation
17 of optimal of 3D STM by using sensitivity analysis obtaining via derivatives of the Von Mises
18 stress fields, finding the force paths prevailing compression in the directions of the strut and
19 the tensile in the directions of the ties for the reinforcement insertion. All the codes are
20 implemented with Matlab software and several comparison examples: Deep beam with
21 opening, a pile cap, a bridge pier, and a single corbel, are presented to validate the present
22 formulations and the results are compared with the literature.

24 *Index terms*— reinforced concrete, topology optimization, strut-and-tie model, SESO, VFLSM.

25 1 I. Introduction

26 In the field of structural engineering, most concrete linear elements are designed by the classical theory of Bernoulli
27 hypothesis. For a real physical analysis about behavior of these bending elements it is common to use the Strut-
28 and-Tie Model (STM) that is a generalization of the classical analogy of the truss beam model. This analogy is
29 shown by Ritter and Morsch at the beginning of the twentieth century, associated with the Reinforced Concrete
30 (RC) beam in an equivalent truss structure (regions B, Fig. ??). The bar elements represent the fields of tensile
31 and the compressed struts emerged inside the structural element as bending effects. The analogy has been
32 improved and is still used by the technical standards in the design of reinforced concrete beams in flexural and
33 shear force and laying down various criteria for determining safe limits in its procedures. However, the application
34 of this hypothesis for any structural element can lead to over or under sizing of certain parts of the structure.

35 The Bernoulli hypothesis is valid for parts of the frame that there is no interference from other regions, such
36 as sections near the columns, changing in geometry or other areas where the influence of strain due to shear
37 efforts is not negligible. In this line, there are regions where the assumptions of Bernoulli do not adequately
38 represent the bending structural behavior and the stress distribution. Structural elements such as beams, walls
39 and pile caps and special areas such as beam-column connection, openings in beams and geometric discontinuities
40 are examples. These regions, denominated "discontinuity regions D", are limited to distances of the dimension
41 order of structural adjacent elements (Saint Venant's principle), that the shear stresses are applicable and the
42 distribution of strains in the cross section is not linear. From the 80's, a Professor at the University of Stuttgart
43 and other collaborators presented several researches that evaluated these regions more adequately, as [1], [2], [3],

5 A) PROBLEM FORMULATION

44 and other researchers as [4], [5] and [6]. The pioneering work by [1] describes the STM more generally, covering
45 the equivalent truss models and including these regions and special structural elements. The analogy used in the
46 STM uses the same idea of the classical theory in order to define bars representing the flow of stress trying to
47 create the shortest and more logical path loads. Several experimental evaluations have been studied to validate
48 the STM applied to the RC design, as [7], [8], [9] and [10].

2 I

50 The STM is recognized as a rational approach to the design of discontinuity regions and is incorporated in several
51 current codes, such as ASCE-ACI 445 on Shear and Torsion [11], [12], [13] and [14]. These code provisions still
52 require improvement due to uncertainties in the selection of optimal struts-and-ties, especially in the case of
53 complex geometry or general load application conditions. Because of its simple model and needs the experience
54 of the designer to select and distribute the elements of the model in order to represent the stresses path in a better
55 way, it becomes evident the use of more reliable and automatic tools for defining its geometric and structural
56 configuration.

3 Fig. 1: D and B regions

58 To overcome these difficulties and improve the efficiency in building the optimal STM in RC structures, the
59 theory of Topology Optimization (TO) has been used for two decades as an alternative and systematic approach
60 consolidating itself as a fruitful path of design related research, once facilitates the shaping of materials under
61 certain conditions. Many methods have been proposed for the solution of TO applied to STM, highlighting the
62 use of the classical SIMP: [15], [16], [17], or ESO (Evolutionary Structural Optimization): [18], [19], [20], Liang
63 et al. [21,22,23], Chen et al. [24], Zhong et al. [25], or variants, like BESO, Shobeiri et al. [26], RESO (Refined
64 ESO), Leu et al. [27] or SESO proposed by the present authors, Almeida et al. [28]. SESO is based on the
65 philosophy that if an element is not really necessary for the structure, its contribution to the structural stiffness
66 is gradually diminished until it does not have any influence in the structure; that is, its removal is done smoothly,
67 not radically as in the ESO method, that have been showed more efficient and robust and less sensitive to the
68 discretization than ESO and faster than BESO, causing a decrease of the checkerboard formation.

69 In the last decade, the Level Set Method (LSM) has been highlighted in the field of TO, different from
70 the conventional element wise density-based methods. LSM has clearer and smoother results and are flexible
71 for complex topological changing, citing the pioneer's works of [29], [30] and [31]. The method describes the
72 topological path by an implicit shape evolutive sequence by using a higher dimensional function to the design
73 space for achieving the minimum energy under design constraints. Several other schemes have been included
74 in the standard LSM to improve performance and achieve better results for general applications, like [32], [33].
75 Wang and Kang [34,35] proposed the Velocity Field Level Set Method (VFLSM) which has been proved to be
76 more efficient to deal with multiple constraints and design variables than LSM, but few works have been applied
77 to STM by using VFLSM.

78 OT in solving problems in the field of 3D STM is not much explored for general D-regions, discouraged by
79 the instabilities (checkerboard problem) inherent to SIMP, ESO/BESO or the complex formulation and high
80 processing time of LSM/VFLSM. Thus, for stabilizing and accelerating the TO solution, several mathematical
81 optimization methods have been proposed, such as Optimality Criteria, by Huang et al. [36] with BESO,
82 Augmented Lagrangian [37] or [38] with Level-Set, Lagrangian multiplier by [39] and [40] with LSM, or the
83 Method of Moving Asymptotes (MMA), by [41] with SIMP.

84 In the present work, aiming at the solution of 3D STM in general reinforced concrete problems, the SESO
85 methods whose advantages are easy implementation and decrease of the checkerboard effect and the VFLSM,
86 which deals well with shape and topological optimizations, are formulated together with the MMA optimization
87 method to accelerate and stabilize 3D STM. It is also noteworthy new approach of sensitivity analysis is
88 incorporated in these formulations for the automatic generation of struts-and-ties based on partial derivatives

4 Global Journal of Researches in Engineering

90 © 2023 Global Journal of Researches in Engineering (GJRE) with respect to Von Mises stresses. The volume constraints are considered in
91 the analyses, as the implementation of a spatial filter and the conjugate gradient method with the incomplete
92 Cholesky preconditioner to speed up the solution of the linear system of each step of the search.

5 a) Problem Formulation

94 Considering the classical topology problem for the maximum stiffness of statically loaded linear elastic structures,
95 a TO mathematical formulation for continuum structure can be discussed. Considering the TO problem as
96 minimizing the deformation energy of a given structure considering the equilibrium, it follows that $W=2U$. The
97 problem can then be defined as: (1) with K_{ij} being the element's elasticity matrix, u_i is the element's
98 strain vector, V is the volume of an element, N is the number of finite elements of the mesh, K is the
99 stiffness matrix, $F = 0$ is the equilibrium equation, F is the vector of loads applied to the structure, u
100 is the design variable of the i -th element, u is the vector of design variables.

162) = ? ????? (??) -?? ?? (?? -1) ????? ?? (??-1) -?? ?? (?? -2) ? < 0 ????? ?? (??) -?? ?? (?? -1) ????? ??
 163 (??-1) -?? ?? (?? -2) ? > 0 ????? ?? (??) -?? ?? (?? -1) ????? ?? (??-1) -?? ?? (?? -2) ? = 0(11)
 164 where the values of ??, ?? and ?? were fitted in the respective numerical ranges 0.65 ? ?? ? 0.75 , 1.15 ? ??
 165 ? 1.25 and 0.9 ? ?? ? 1.

166 It can be seen in Eq. (11) that the MMA saves the signal of three consecutive iterations. Thus, when the
 167 signals alternate, the MMA detects that the values of the design variables are oscillating, i.e., ??? ?? (??)
 168 -approximate the design point ?? ?? (??) . If the values of the design variables do not oscillate, i.e., ??? ??
 169 (??) -?? ?? (?? -1) ????? ?? (??-1) -?? ?? (??-2) ? ? 0, then the MMA moves the asymptotes away from the
 170 design point in order to accelerate up convergence. There are two approaches to solving subproblems in MMA,
 171 the "dual approach" and the "primal-dual interior point approach". The dual approach is based on the dual
 172 Lagrangian relaxation corresponding to the subproblem, which seeks the maximization of a concave objective
 173 function without other constraints and the non-negativity condition on the variables. This dual problem can be
 174 solved by a modified Newton method, and then the dual optimal solution can be translated into a corresponding
 175 optimal solution of the primal subproblem, which is used in this paper.

176 8 III. Methodology for Generation 3D Strut-and-Tie Models 177 and the Final Flowchart

178 To determine the path load of the 3D bars of the STM from the TO analysis, this paper employs a new procedure
 179 to evaluate the struts and ties by the signs of the derivatives of the Von Mises stress components. It is known
 180 that for 3D problems they can be written as $(\sigma_{ij})^2 = 1/2 [(\sigma_{11} - \sigma_{22})^2 + (\sigma_{11} + \sigma_{22})^2 - 2\sigma_{11}\sigma_{22}]$
 181 ? , < 0 the asymptotes ?????????????? -? ??? ?? (??) -?? ?? (??) ? 2 ?? ?? -?? ?? (??) ????? ????? ?? ??? ?
 182 (??) ? ?? 1 ?????????????? ????? ?? ? ?? ?? -?? ? 0 ?? ? ?? ?

183 Taking the local calculation of the derivative of the von Mises stress of the element with respect to the
 184 components of the stress vector described respectively as: $\partial \sigma_{ij} / \partial \sigma_{11} = 1/2 [(\sigma_{11} - \sigma_{22}) / (\sigma_{11} + \sigma_{22})]$
 185 -?? ??22 -?? ??33) ??(?? ??) / (??22 + ??33) = 1/2 [?? - ??] / (?? + ??) (??22 -?? ??11 -?? ??33) ??(?? ??) / (??22 + ??33)
 186 ????? ??33 = 1/2 [?? - ??] / (?? + ??) (??22 -?? ??11 -?? ??33) ??(?? ??) / (??22 + ??33) = 3/2 [?? - ??] / (?? + ??)
 187 ??(?? ??) / (??22 + ??33) = 3/2 [?? - ??] / (?? + ??) (??22 -?? ??11 -?? ??33) ??(?? ??) / (??22 + ??33) = 3/2 [?? - ??] / (?? + ??)

188 Considering Eq.(??3) and making??(?? ??) / (?? + ??) = 1/2 [?? - ??] / (?? + ??)
 189 > 0 then the elements are preponderantly tensioned (blue color -ties) while??(?? ??) / (?? + ??) = 1/2 [?? - ??] / (?? + ??)
 190 < 0 are preponderantly compressed (green color -strut). The flowchart presented in Fig. ?? shows the original
 191 methodology presented in this section with the approach of using element sensitivity for automatic generation of
 192 STMs via stress derivatives, when a target volume is reached, the stopping criterion is reached. A set of techniques
 193 has not yet been presented in scientific articles on 3D models, so the results obtained in item 4 are compared
 194 with those proposed by [16], [26] and [45]. Highlights that the VFLSM method required a neighborhood filter to
 195 define the tensile (blue) and compression (green) regions. This filter is due to intermediate values that occur in
 196 continuous TO methods such as the intermediate densities that occur in the SIMP methodology.

197 9 IV. Numerical Examples

198 The following examples of structures engineering focus on TO base on minimizing compliance for STMs. The
 199 geometry and boundary conditions for numerical applications are represented for each case. All numerical
 200 examples were processed on a Core i7-2370, 8th Gen notebook, 2.8 GHz CPU with 20.0 GB (RAM).

201 10 a) Example 1 -Deep Beam with Opening

202 The example presents a simply supported deep beam with an opening at the bottom left corner. The beam
 203 has its span three times its height and it is defined in [46], where the simple bending structural behavior is no
 204 longer considered. A vertical downward force F=3000 kN is applied eccentrically at the top edge as shown in
 205 Fig. ???. The structure is discretized with a total of 65,420 hexahedral elements (SESO) and 65,420 tetrahedral
 206 elements (LSM) (Fig. ?? shows the design domain and its boundary conditions). In this configuration, the force
 207 in off-center position and the opening positioned near the left low end create a situation that changes the internal
 208 stress flow in the structure, between the load and the supports. The tie elements, resulting from tensile stresses,
 209 are positioned at the extremities of the strut elements, resulting from compressive stresses, geometrically defining
 210 the final model. Fig. 6 provides the optimal topologies of the optimization procedures for the SESO (Fig. 6a and
 211 Fig. 6b) and VFLSM (Fig. 6c) methods, with a final volume fraction equal to 32%. The optimal configurations
 212 have similarity to the classical STM presented by [1] and later by [20]. The computational cost presented by
 213 SESO using Optimality Criteria [47] is approximately 40% lower than the SESO and VFLSM methods using the
 214 MMA. It can be also noticed in Fig. 6 that the optimal settings obtained by the VFLSM formulation clearly
 215 defines distinct elements (strut or tie) near the lateral faces of the deep beam, resulting in a more discrete STM,
 216 compared to the optimal settings presented by the SESO method. The classic model, Fig. 7, denotes three
 217 diagonal struts starting from the region of load application, one of them external directed to the closest support,
 218 another contouring the opening and directed to the support, and a third internal one. The ends of the struts
 219 are connected by tie composing the final structure of the STM. [45] In Fig. 8 it can be seen that the SESO

formulation (Fig. 8a) results in a setting similar to the classical model, but the VFSLM formulation (Fig. 8b) presents a model with a discretely simpler setting, with the internal strut in the vertical direction, unifying at a lower point the two ties. This setting simplifies the design procedure and the reinforcement detailing of the reinforced concrete structure, in the practical and executive sense, although the classic model makes it possible to calculate the complementary reinforcement around the opening.

11 b) Example 2 -Pile Cap

In this example, a building foundation structure is dimensioned as a pile cap according to the dimensions shown in Fig. 9, for consideration as a rigid block and to enable the analysis by the STM concept. The pile cap is subjected to a vertical force of 4,000 kN located at the center of the upper face. The material properties used are the compressive strength of the concrete cylinder is 32 MPa. The Young's modulus of the concrete $E_c = 25,000$ MPa and Poisson's coefficient $\nu = 0.15$. The filter radius $r_f = 1.5$ mm and the volume fraction of 22.5%, a rejection ratio, $RR = 1\%$ and the evolution ratio $ER = 2\%$ were specified in the optimization process.

12 Global Journal of Researches in Engineering

© 2023 Global Journals In the numerical simulations, to discretize the domain of the structure, a refined mesh of $40 \times 20 \times 40$ was used, totaling 32,000 hexahedral elements (SESO) with 1mm reference side was used and a mesh of 32,000 tetrahedral elements (VFSLM). The results obtained as final optimal topologies of this problem for these meshes are represented in Fig. 10 and can be compared with the results with those presented by [16] and [26], see Fig. 11.

The optimal topology is basically composed of discrete elements represented in the principal stress flows. These optimal settings are adequate to perform the detailing and dimensioning of the required reinforcement, as well as strength checks. In this structure, the vertical load is distributed in four struts inclined toward the supports represented by vertical piles. The models highlight elements at the base of the pile cap, representing the tensile stresses, where a plane frame of ties balances the strut ends generated by the 3D structure in both horizontal directions, Fig. 10, where it can be seen the optimum topologies for the two methods, SESO and VFSLM. In the automatic generation of the strut models, it was considered the main flows of distinct stresses by colors, where the region of compression struts is green color and the region of tensile ties is blue. Although the models result quite similar, when approaching this problem, one must consider the increased computational burden associated with a 3D structure; a solid mesh usually requires that many elements be investigated at an adequate level of detail, with notable consequences on the number of equations and variables. Seeking to minimize this aspect of the processing, the system of equations received the implementation of a sparse approximation preconditioner for the inverse matrix. With this routine active, the computational cost of SESO-3D for this problem was decreased from 8,000 sec to 1,854 sec (4.3 times less) while VFSLM had a decrease from 8,000 sec to 3,851sec (2.1 times less).

The dimensioning of the reinforcement of this model is performed, as already presented in [28]; in the calculations of the dimensions of the model elements, namely, inclined compression strut -column-pile and horizontal tension tie -pile-pile, the geometry of the problem presented [26] is used: In the inclined strut, the verification of the compressive stresses is performed according to and the area of the strut required for the design strength of the concrete not to be exceeded: $\sigma_c \leq f_{cd}$ $A_{st} = \frac{N}{\sigma_c} = \frac{1.4 \cdot 2,031}{0.8 \cdot (3.2/1.4)} = 1.555$ $A_{st} = 1.555$

By way of comparison, in [26], the results of this sizing are $A_{st} = 41.66$ and $A_{st} = 1,659$. The differences in values (3.5% and 6.3, respectively) are due to different calculation criteria between the technical standards used, but values of the same order of magnitude can be considered. Fig. 12 shows the reinforcement arrangement for the pile cap. The SESO and VFSLM methods using the MMA as accelerator are applied to a structure representing a column receiving loading from the bridge superstructure, represented by four vertical forces, as shown in Fig. 13. The concrete material properties, rejection ratio (RR), evolutionary ratio (ER) and filter radius are the same as in the previous example. For the numerical simulations, in the SESO method the bridge support is discretized using a fine mesh of $85 \times 55 \times 20$ hexahedral elements of eight nodes, with reference side of 1 mm, while in the VFSLM method the mesh used has $85 \times 20 \times 55$, totaling 93,500 tetrahedral finite elements.

13 Global Journal of Researches in Engineering

The compliance history and the performance of the methods during the optimization procedure are plotted in Fig. 14. It can be seen in Fig. 14b that the performance index perfectly captures the changes in compliance and increases from unity to a maximum value of 2.3, stabilizing quickly around 2.1, the value at the optimal iteration.

The history of the optimization procedure via SESO and VFSLM for the bridge pier are shown in Fig. 15 and Fig. 16. The optimal topologies were achieved at iterations 82 and 100 with final volumes equal to 20% of the initial volume and a computational cost of 4,315.8 sec for SESO while VFSLM showed a computational cost of 5,486.5 sec. The optimal settings with highlights of the distinct regions by colors are presented in Fig. 17 for the two methods proposed in this paper. In these representations, a vertical axial force is expected to balance the

279 symmetric external loads in the region of the base constraint. The applied vertical forces, in fact, are transferred
280 to the column axis by means of two inclined struts and two vertical struts that merge into two in the proximity
281 of the top region of the vertical element, driving the load distribution to the lower region where are the base
282 supports. Note that the SESO method creates a unified region at the base while the VFLSM method sets up
283 two parallel vertical paths. In addition, a horizontal tensile tie is arranged at the top of the body receiving the
284 applied forces, which ensures the "T" geometry of the structure and configures the struts equilibrium in the load
285 application zones. From a numerical point of view, the result obtained is optimal and configures the symmetry
286 defined by the position of the design load. For automatic generation of STM models in the VFLSM method,
287 it was necessary to implement the derivatives of von Mises stresses in the code proposed by [34]. stress flows
288 (green) similar to those of the SESO method, Fig. 17a, highlighting the robustness of both methods for creating
289 strut-and-tie models. With the objective of investigate the effects of D-regions, three holes were inserted in the
290 horizontal element of the bridge pier structure, and the number of finite elements of the mesh was reduced to
291 88,700, as shown in Fig. 18. The optimal topologies of the SESO and VFLSM models are represented in Fig.
292 19, where the struts are represented by green color and the ties by blue color.

293 The optimum results obtained demonstrate that the presence of geometric discontinuities produces changes in
294 the stress flows, that seek to contour the discontinuities, describing practically vertical struts in the horizontal
295 body of the bridge pier from the points of load application. These struts bend below the openings to meet at the
296 top of the vertical element, creating points of deviation that need to be equilibrated by tensile ties. In Fig. 19,
297 it can be seen the representations of STM elements created as described.

298 This modification with the presence of the openings affects the STMs models significantly, and the real load
299 transfer mechanism can change with the dimensions of the openings. The optimization histories are shown in Fig.
300 ??0 and Fig. ??1, by the SESO and VFLSM formulations, respectively. The SESO and VFLSM methods were
301 also experimented with for modeling struts-and-ties in a single corbel attached to a column. A simple structure
302 can eventually result in an intricate STM as the dimensions and load arrangements can be defined. The geometry
303 and dimensions of the structure are shown in Fig. ??2. This single corbel is subjected to a concentrated load of 1
304 kN. The compressive strength of the concrete used in this example is 32 MPa. Young's modulus of the concrete
305 $E = 28,567$ MPa and the Poisson's ratio $\nu = 0.15$ were defined in the analysis. A prescribed fraction volume V
306 $= 0.22$ m³ and an evolution ratio of $ER = 2\%$ was specified in the optimization process.

307 In the SESO method the structure was discretized with a mesh of $44 \times 12 \times 108$ unit hexahedral finite elements.
308 The performance of the structure was monitored throughout the optimization procedure and, despite the breaks
309 in the load transfer mechanisms due to element removal, the structure did not present failure modes and the
310 performance index remained higher than 1, stabilizing at 1.6. In the VFLSM method, the same mesh was used,
311 totaling 57,024 tetrahedral elements. Figures 23a, b, c and ?? show that the optimal topologies obtained by
312 the two models are different and checkerboard patterns were not detected. It is noted in observation made in
313 the deep beam example that both formulations, SESO and VFLSM, define settings differently for elements of
314 strut-and-tie models. Discrete elements are configured on the side faces of the models

315 14 Global Journal of Researches in Engineering

316 © 2023 Global Journals () in different regions, while complete planes are shaped in other regions, with no
317 common convention between the two formulations. The presented results show that both SESO-3D and VFLSM-
318 3D are able to provide the prediction of the load transfer mechanism in reinforced concrete structures, even
319 considering the structural domain thickness in the configuration of the component elements of the models. The
320 STMs are presented in Fig. 24, it can be seen that these models are different and capable of clearly representing
321 the location of the struts, ties and nodal zones. These results can be compared with those presented by [16] and
322 [26]. It is also highlighted that the parameters of the MMA optimizer were changed to $\alpha = 0.98$, $\beta = 1.25 \times 10^{-4}$
323 $\gamma = 0.75$ proportion a more feasible topology for design. Fig. 24b shows the optimal setting of the VFLSM
324 used for automatic creation of the STM models; both formulations exhibit distinct tensile (blue) and compressed
325 (green) regions, even in the width of the structural domain. Table 1 highlights the computational cost of SESO
326 and VFLSM in all the examples presented in this paper evidencing the better performance for SESO-OC and
327 SESO-MMA compared to VFLSM-MMA. This paper aimed to extend the application of TO in 3D elasticity to
328 obtain the best solution to STM problems. It brought some processes as innovation, such as the use of the SESO
329 method and the VFLSM employed in conjunction with the OC and MMA methods to accelerate and stabilize
330 the analyses; so that, the first method demonstrated to be more efficient when employed with the SESO, about
331 2 to 3 times faster in all the examples evaluated. It is highlighted that in these processes the incorporation
332 of the linear solution by the conjugate gradient method with the incomplete Cholesky preconditioner further
333 enhanced the computational cost. In the automated generation of the final designs of the STM, the procedure
334 of obtaining struts and ties computed by the partial derivatives of the stresses of each element was applied
335 highlighting that this novelty is easy to implement and the use of a spatial modal filter in the stress field was
336 enough to completely eliminate the checkerboard. From the automatic generations performed, it was possible to
337 design an example according to the recurring norm in an expeditious manner, in which the required reinforcement
338 areas were evaluated and compared, demonstrating a good similarity. All codes were implemented in the high
339 level language Matlab, which is easily accessible and extensible for future incorporation of other more realistic
340 models, such as a rheological model more suitable for concrete. The study of STM using optimization applied to

341 both materials (steel and concrete), leading to dimensioning and detailing of RC structural elements under the
 342 reliability-based topology optimization (RBTO) paradigm, taking advantage of the efficiency and stability of the
 procedures, are the highlights in the formulations developed in this paper. ^{1 2}

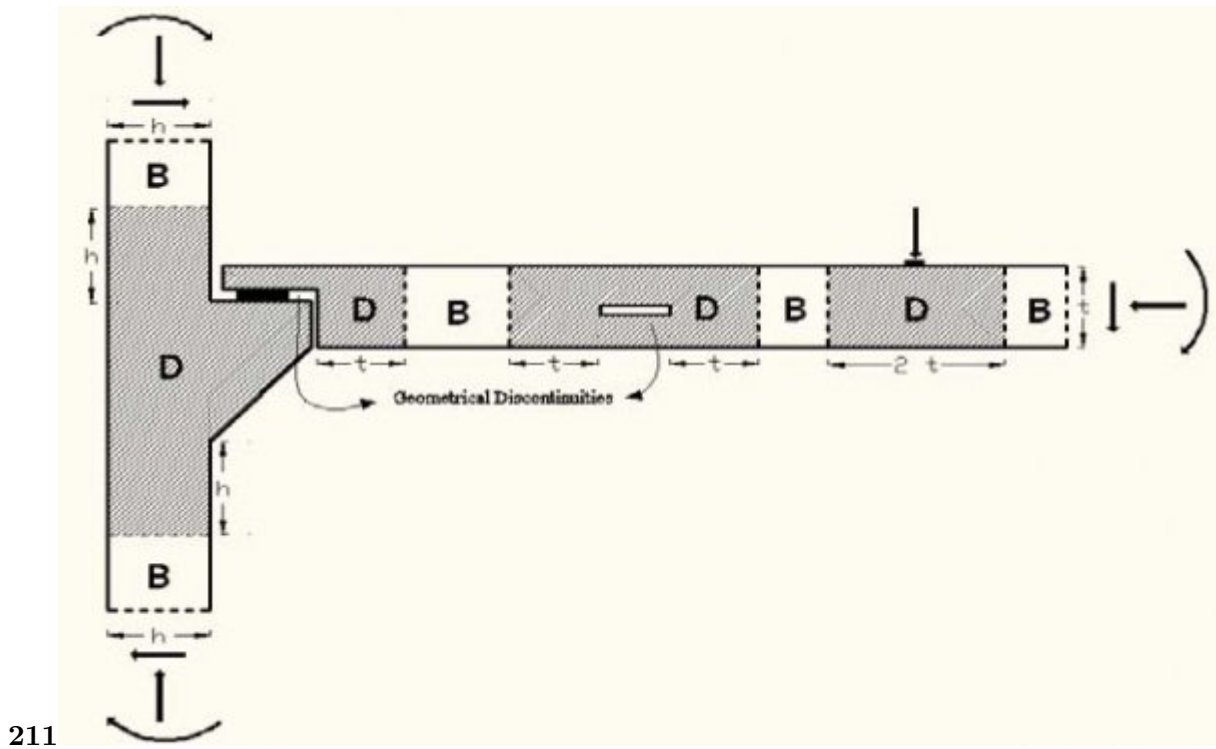


Figure 1: Fig. 2 : 1 2 1 2

343

¹ Topology Optimization: Applications of VFSLM and SESO in the Generation of Three-Dimensional Strut-and-Tie Models

² Year 2023 Topology Optimization: Applications of VFSLM and SESO in the Generation of Three-Dimensional Strut-and-Tie Models

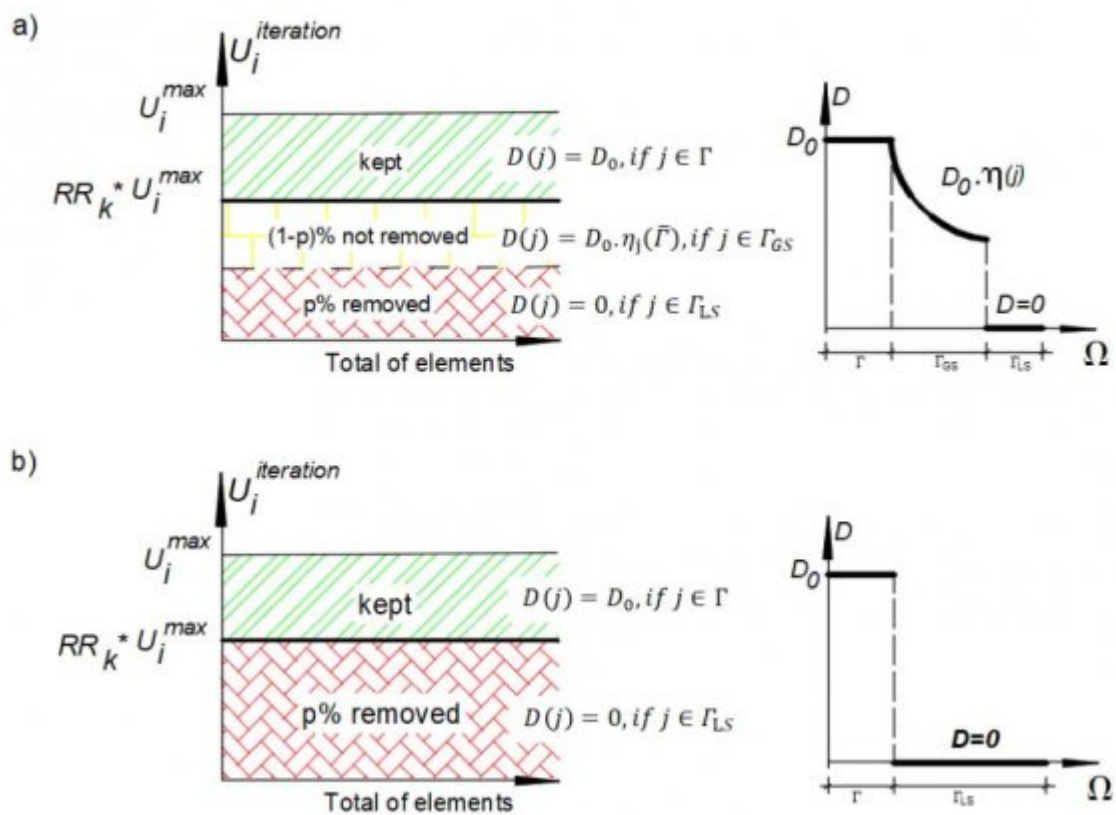


Figure 2:

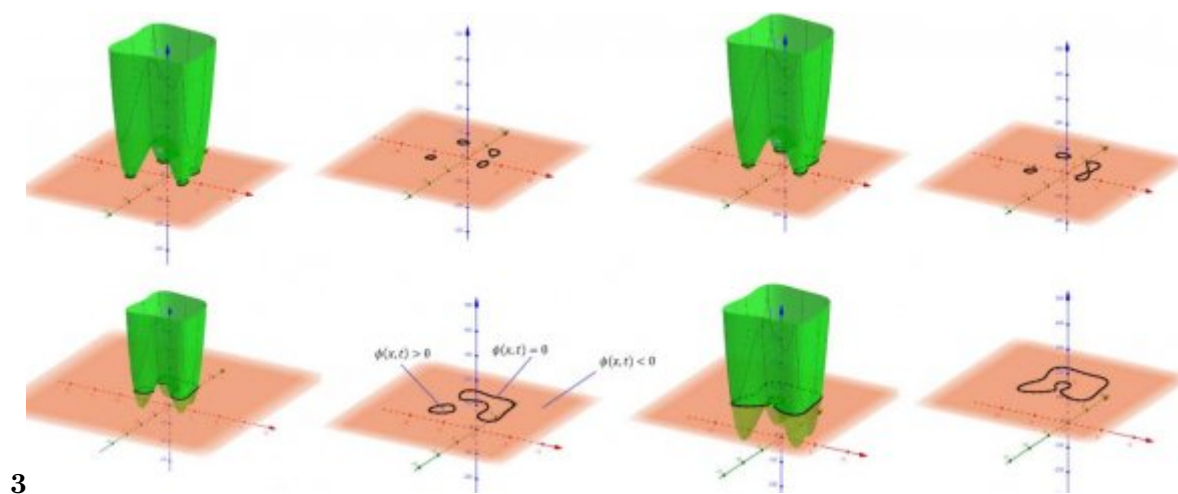
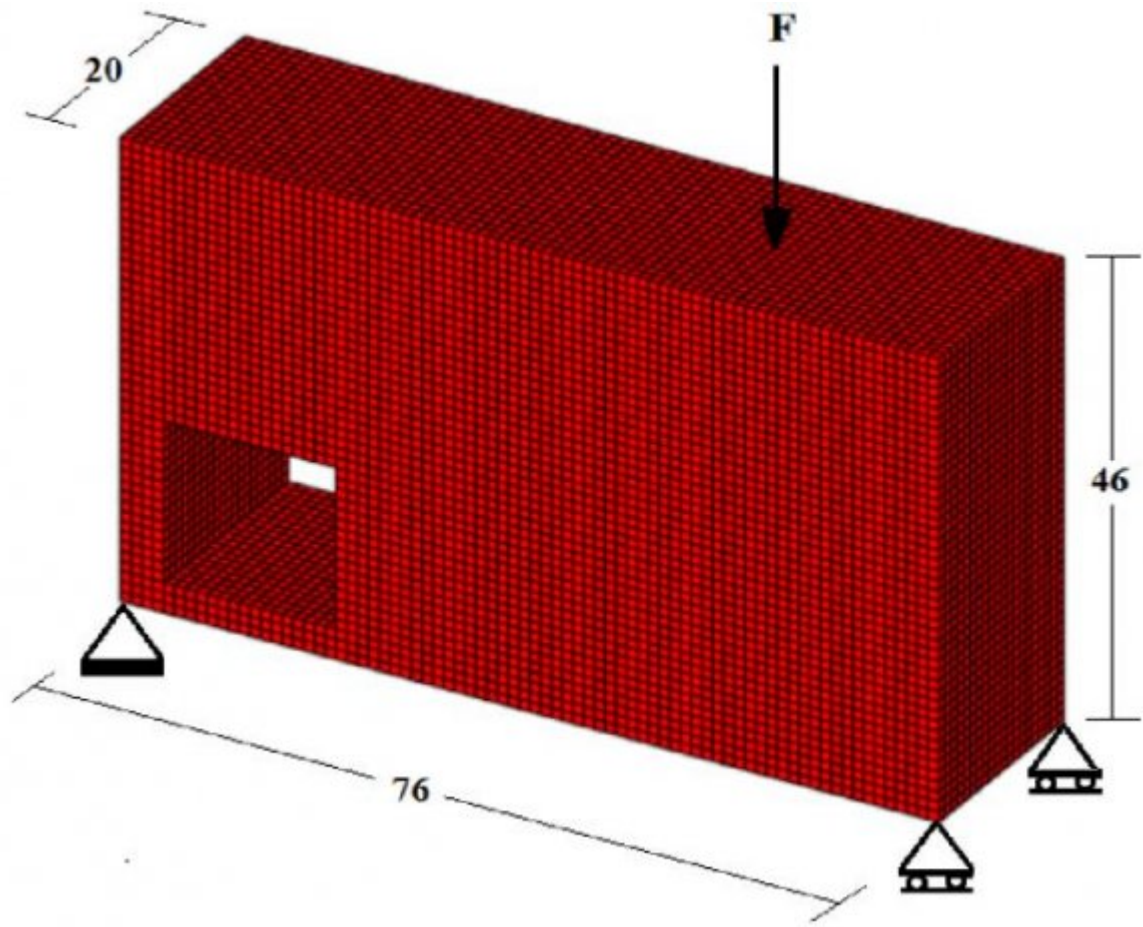
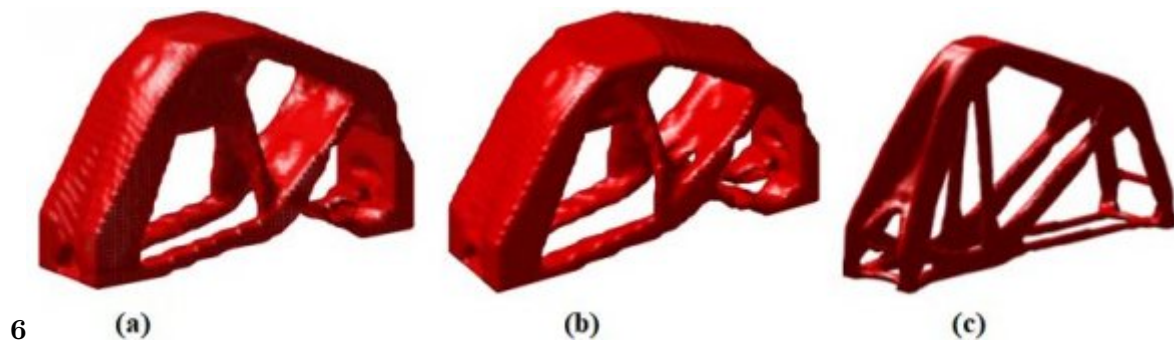


Figure 3: Fig. 3 :



45

Figure 4: Fig. 4 :Fig. 5 :



6

(a)

(b)

(c)

Figure 5: Fig. 6 :

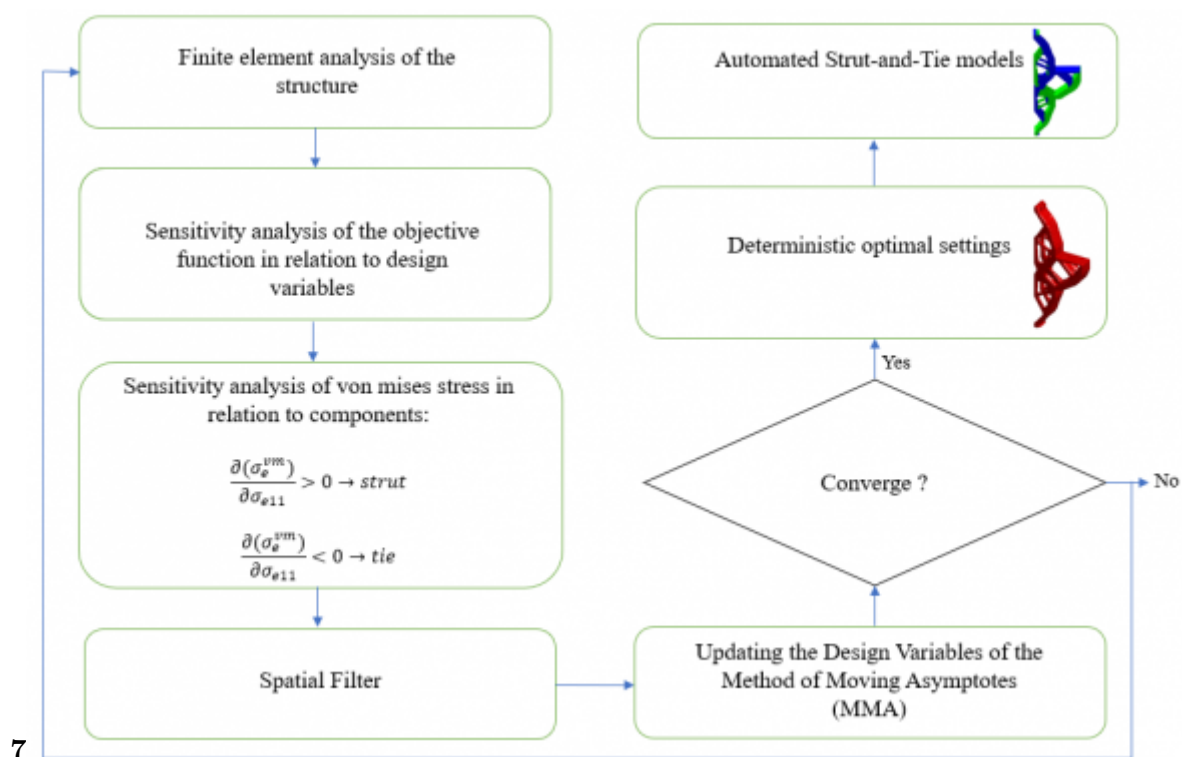


Figure 6: Fig. 7 :

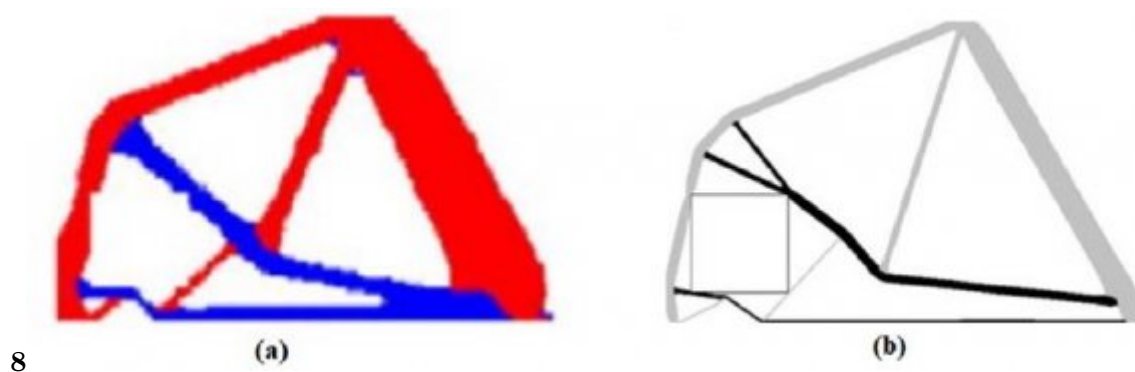


Figure 7: Fig. 8 :

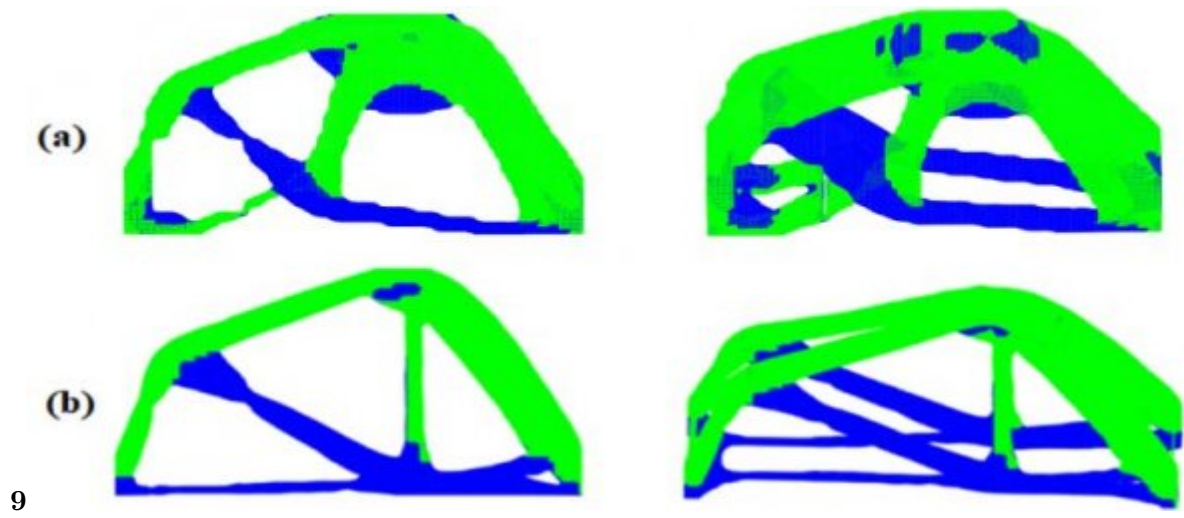
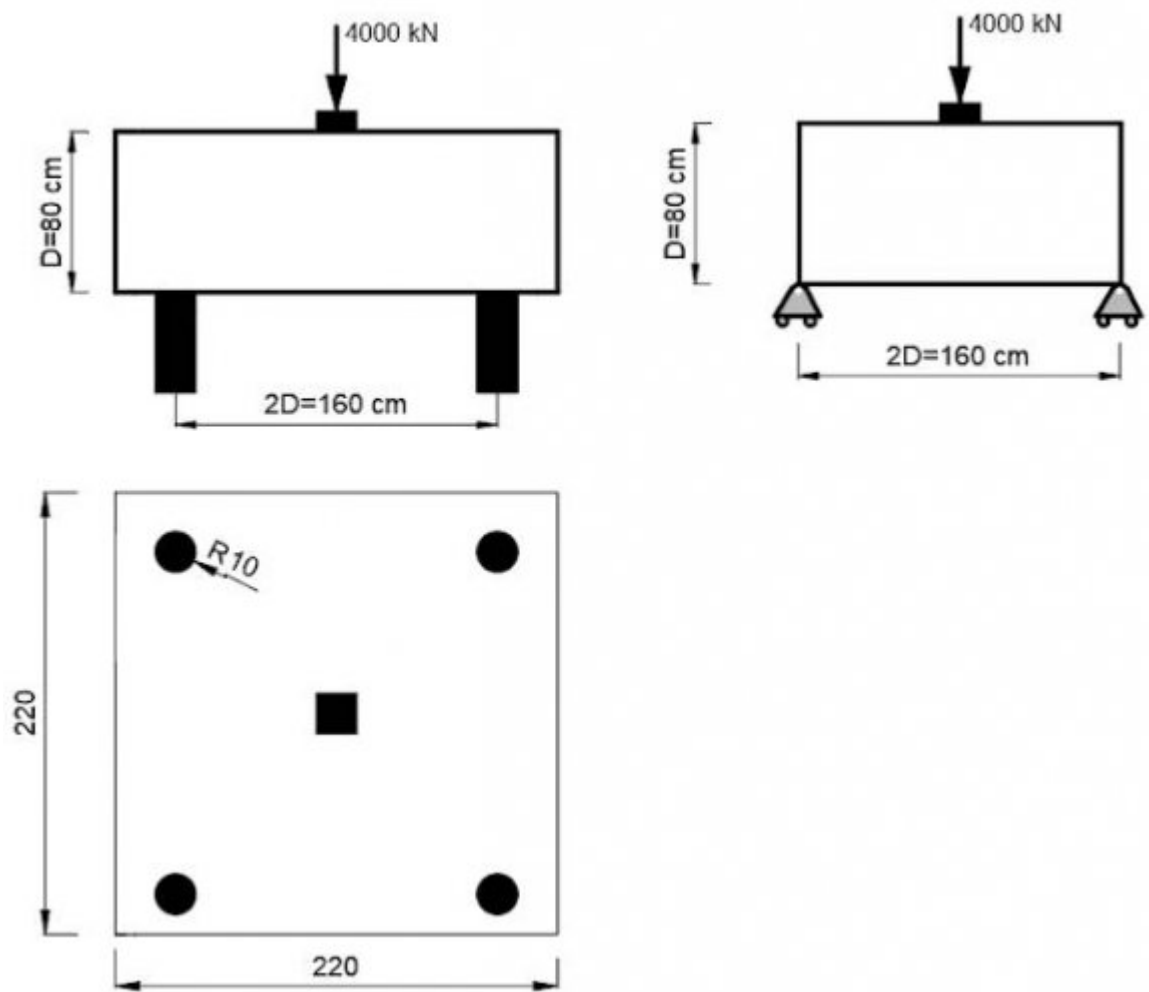


Figure 8: Fig. 9 :

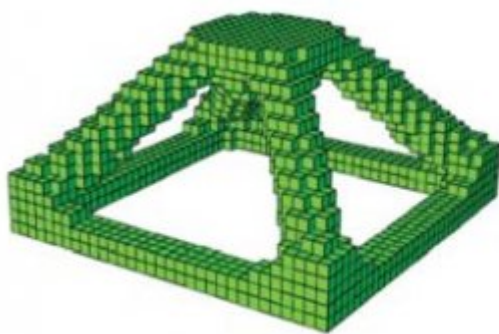


1011

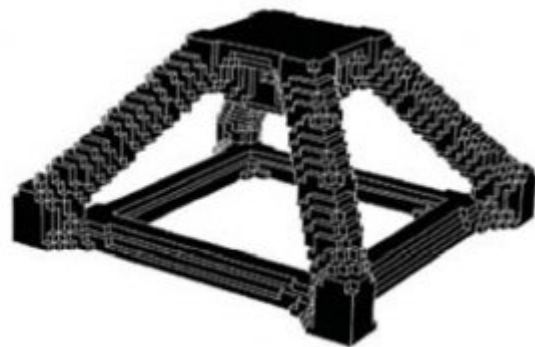
Figure 9: Fig. 10 :Fig. 11 :



Figure 10:



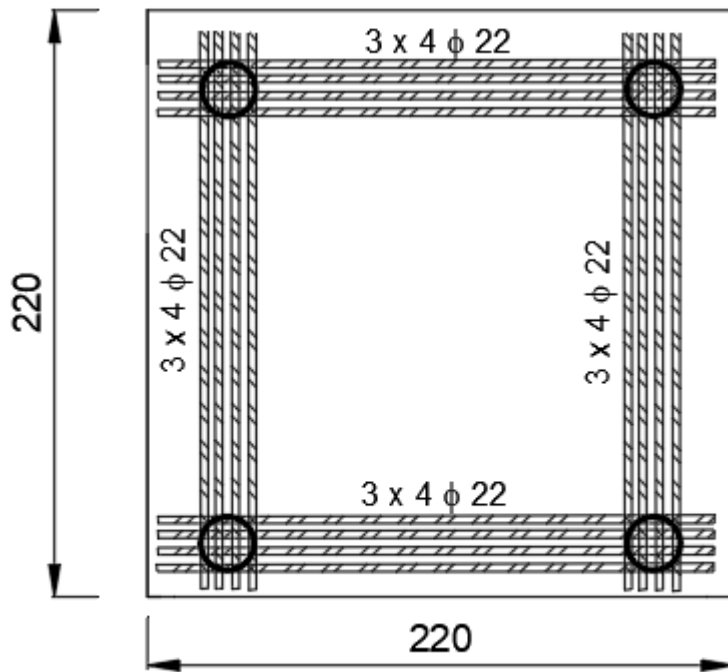
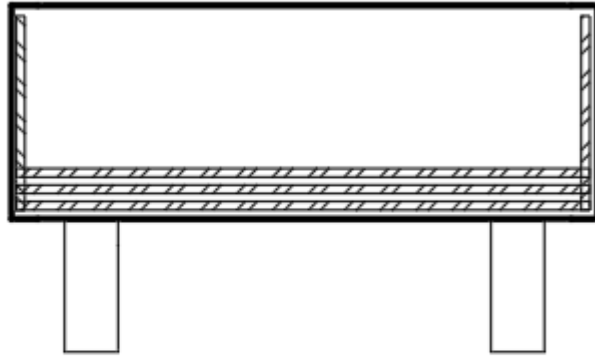
(a)



(b)

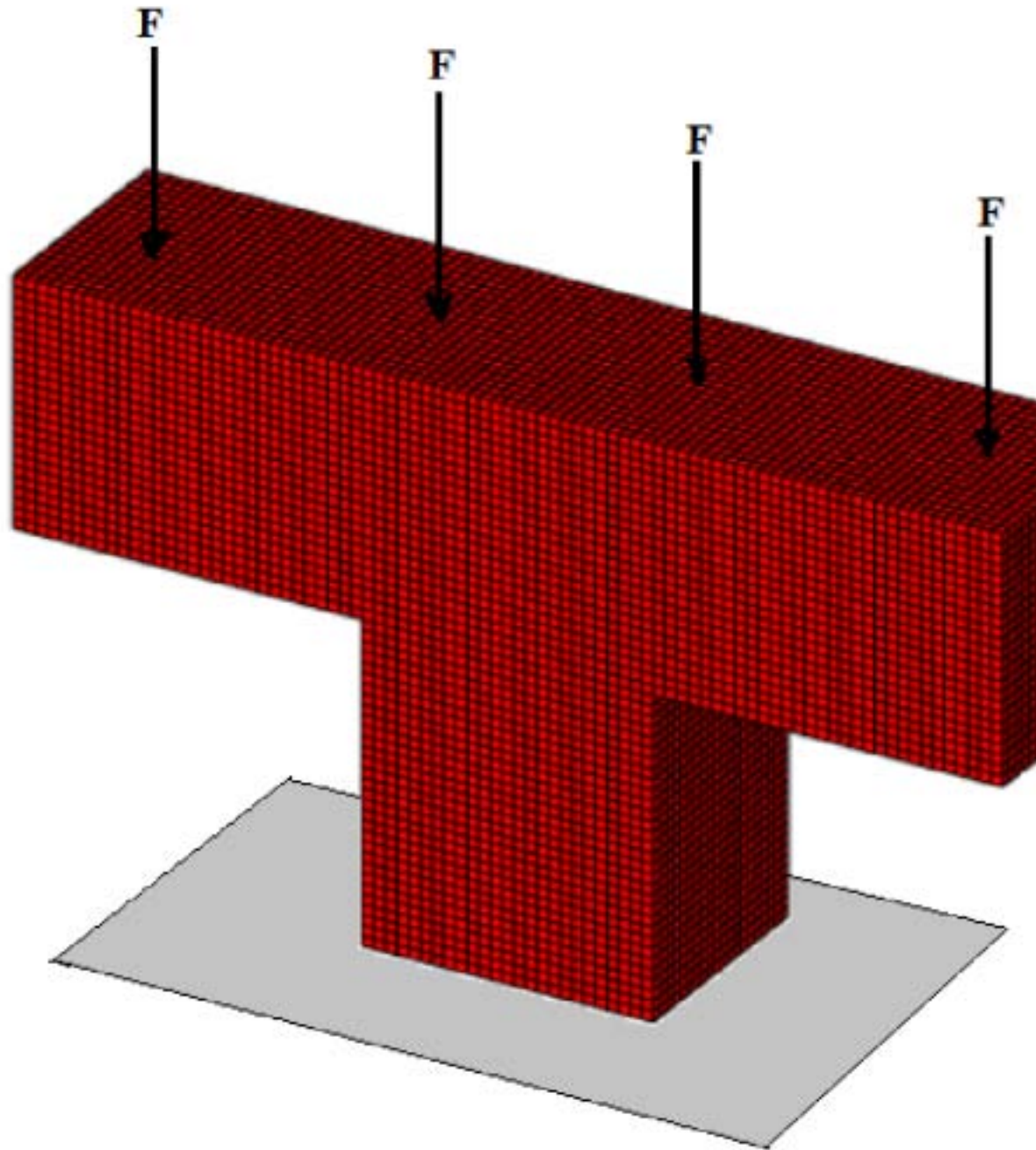
12

Figure 11: Fig. 12 :



13

Figure 12: Fig. 13 :



141516

Figure 13: Fig. 14 :Fig. 15 :Fig. 16 :

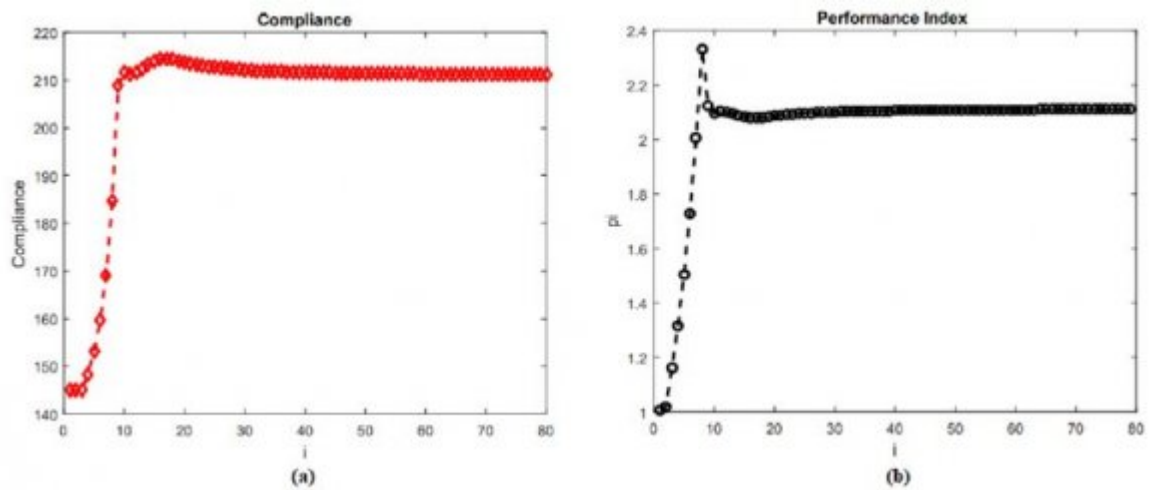
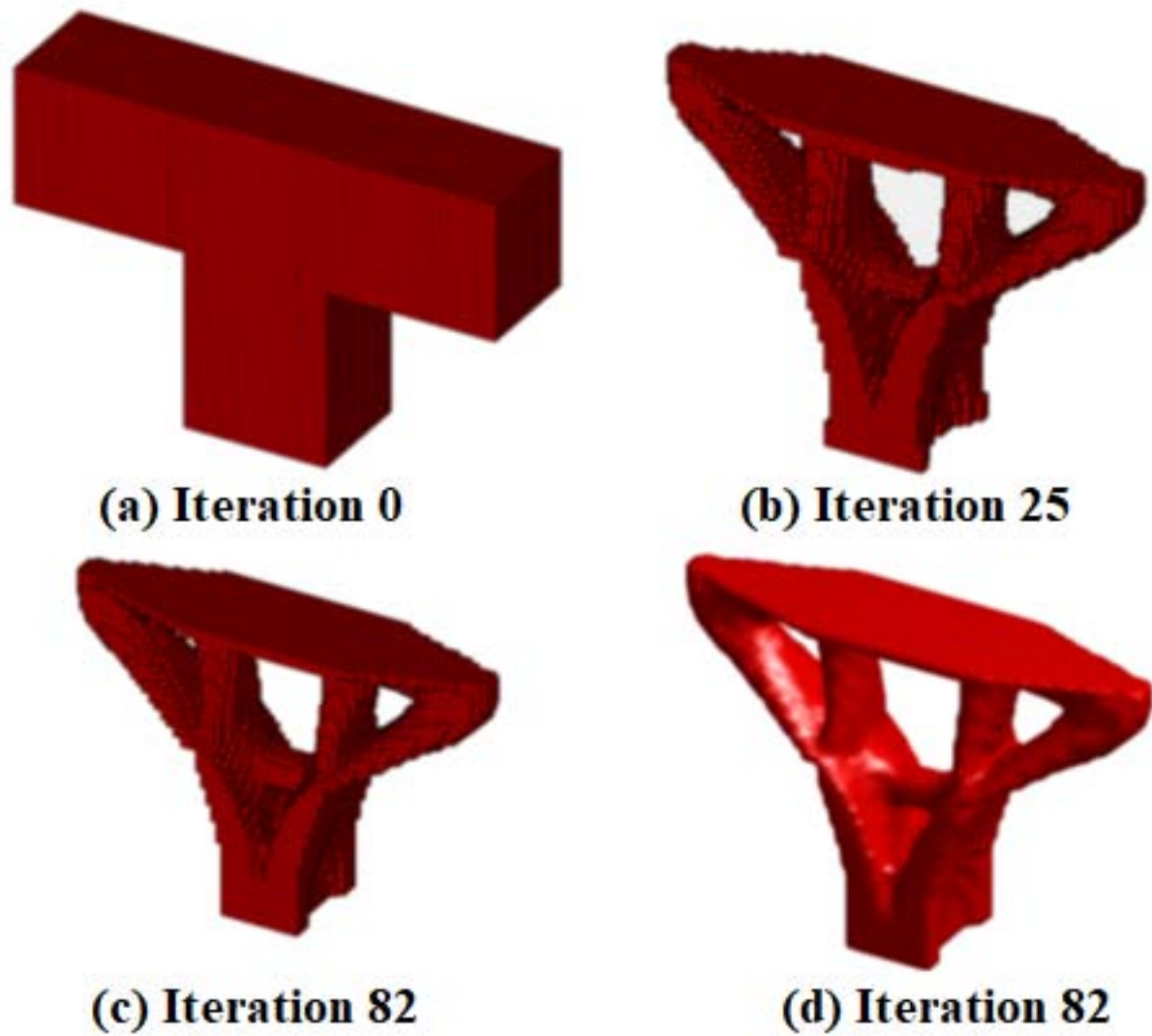
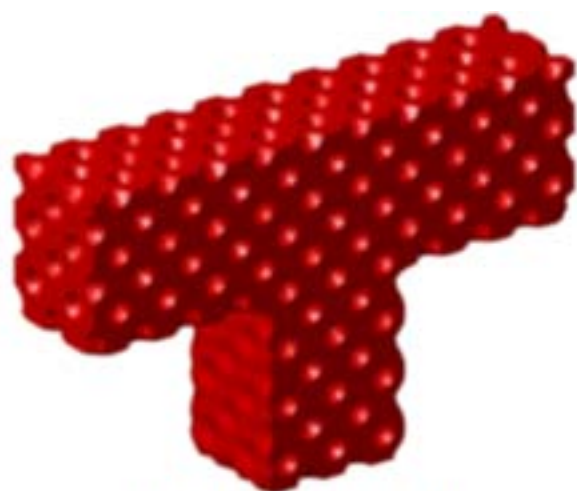


Figure 14:



17182021

Figure 15: Fig. 17 :Fig. 18 :Fig. 20 :Fig. 21 :



(a) Iteration 0



(b) Iteration 25



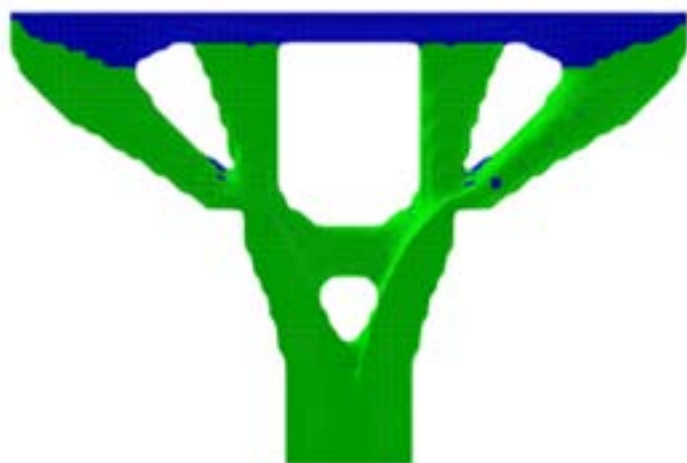
(c) Iteration 68



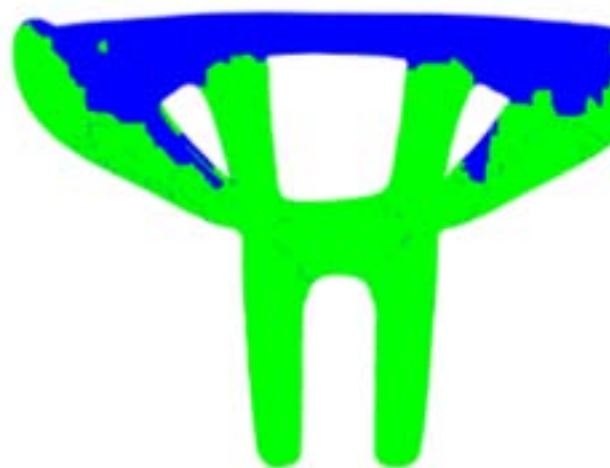
(d) Iteration 100

2223

Figure 16: Fig. 22 :Fig. 23 :



(a)



(b)

24

Figure 17: Fig. 24 :

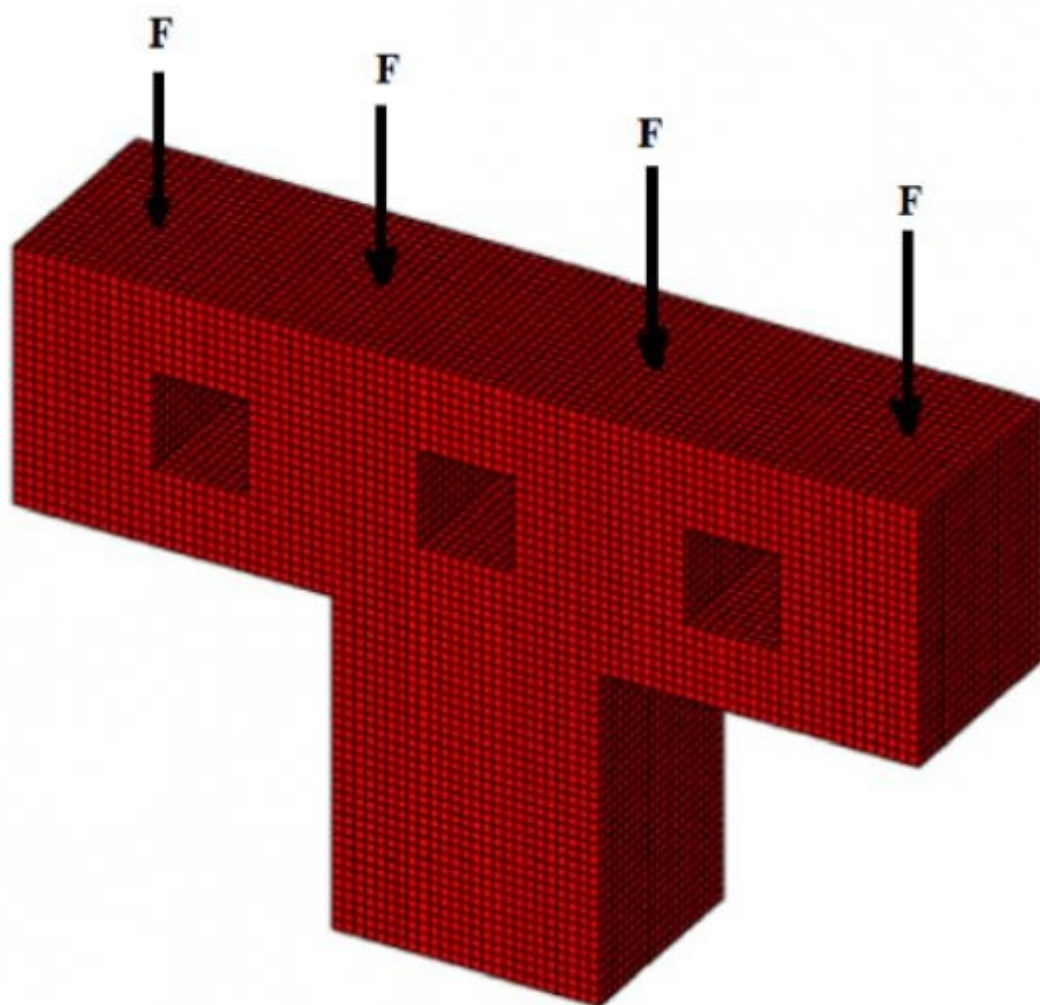


Figure 18:

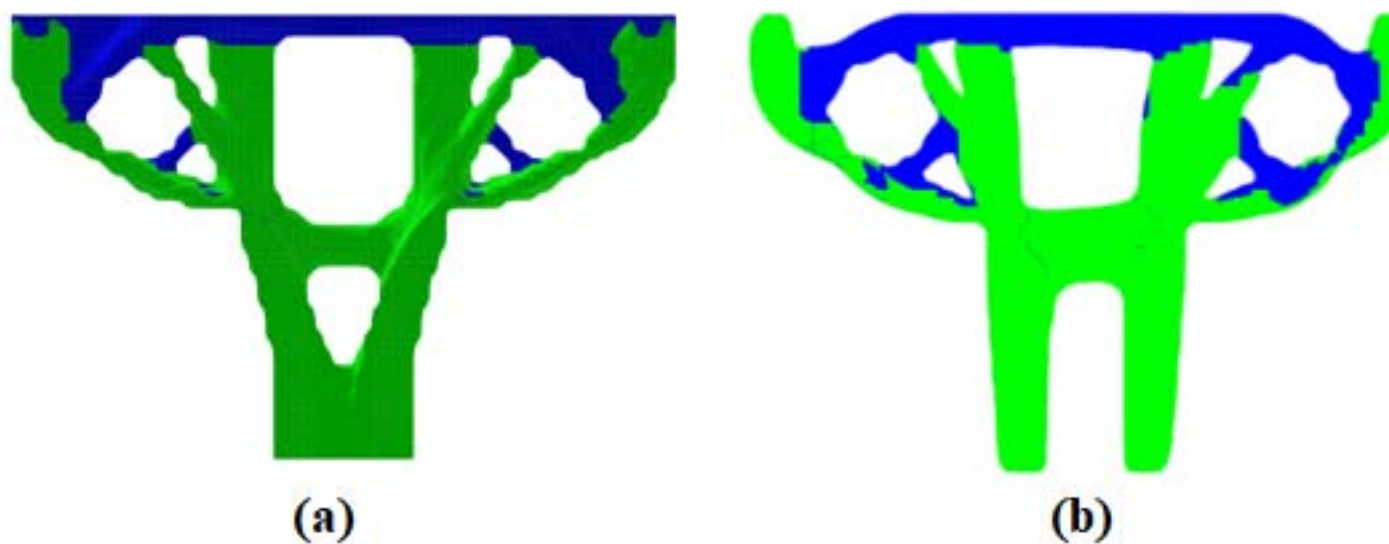
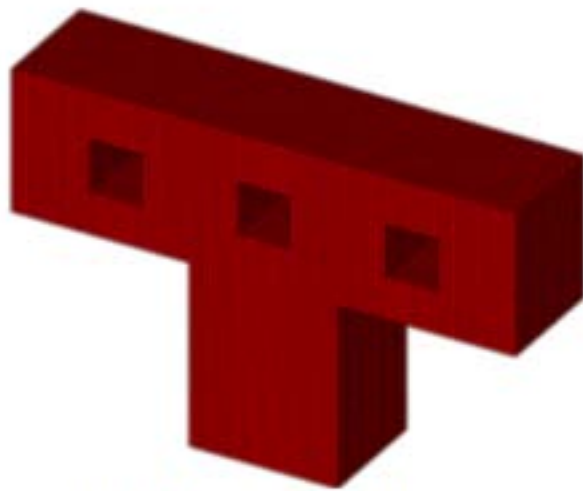
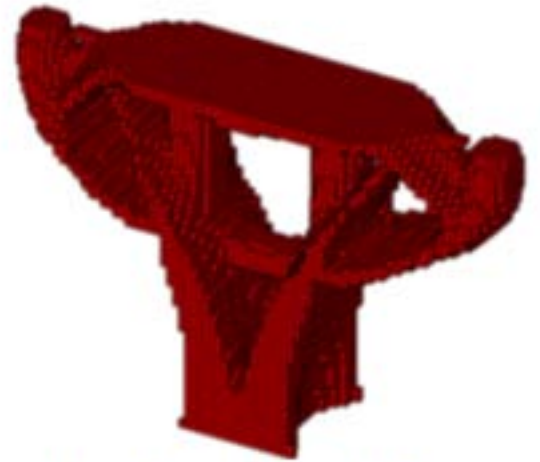


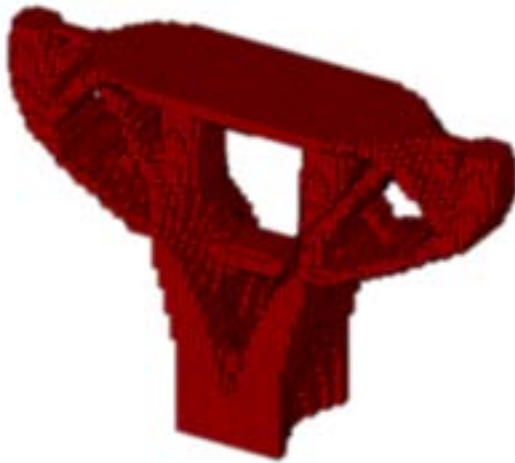
Figure 19:



(a) Iteration 0



(b) Iteration 25



(c) Iteration 82



(d) Iteration 82

Figure 20:

Year 2023
27
Volume Xx XIII Issue II V ersion I
() E
Global Journal of Researches in Engineering
(12)
2 + ?? 23 2
+ ?? 31 2)
© 2023 Global Journ als

Figure 21:

1

Structure	Computational Cost (SESOC) (minute)	Computational Cost (SESOMMA) (minute)	Computational Cost (VFLSM) (minute)	Strut-and-tie Models
Deep beam with opening	90.7	109.8	229.81	
Pile Cap	21.4	38.0	64.2	
Bridge pier	57.9	95.0	159.3	
Bridge pier with three holes	56.5	95.9	158.6	
Single Corbel	45.4	71.9	103.7	

Global Journal of Researches in Engineering© 2023 Global Journals () E Volume Xx XIII Issue II Version I 38 Year 2023

Figure 22: Table 1 :

1 Acknowledgment

- The authors acknowledge the Sao Paulo State Research Foundation (FAPESP) under Grant Number 2016/02327-5 for their financial support and CNPq (National Council of Scientific and Technological Development) under Grant Numbers 305093/2018-5 and Federal Institute of Education, Science and Technology of Minas Gerais under Grant Numbers 23792.001327/2022-49.
- [Yamasaki et al. ()] ‘A level set based topology optimization method using the discretized signed distance function as the design variables’. S Yamasaki , T Nomura , A Kawamoto , K Sato , K Izui , S Nishiwaki . *Struct Multidisc Optim* 2009. 41 (5) p. .
- [Luo et al. ()] ‘A level set method for structural shape and topology optimization using radial basis functions’. Z Luo , L Tong , Z Kang . *Comput Struct* 2009. 87 p. .
- [Wang et al. ()] ‘A level set method for structural topology optimization’. M Y Wang , X Wang , D Guo . *Comput Methods Appl Mech Eng* 2003. 192 p. .
- [Zhong et al. ()] ‘A new evaluation procedure for the strut-and-tie models of the disturbed regions of reinforced concrete structures’. J T Zhong , L Wang , P Deng , M Zhou . *Engineering Structures* 2017. 148 p. .
- [Xie and Steven ()] ‘A simple evolutionary procedure for structural optimization’. Y M Xie , G P Steven . *Computers & Structures* 1993. 49 (5) p. .
- [Simonetti et al. ()] ‘A smooth evolutionary structural optimization procedure applied to plane stress problem’. H L Simonetti , V S Almeida , L O Neto . *Eng Struct* 2014. 75 p. .
- [AASHTO LRFD Bridge Design Specifications; American Association of State Highway and Transportation Officials ()] *AASHTO LRFD Bridge Design Specifications; American Association of State Highway and Transportation Officials*, 2007. Washington, DC, USA: American Association of State Highway and Transportation Officials.
- [Vaquero and Bertero (2020)] ‘Automatic Generation of Proper Strut-and-Tie Model’. Sebastian F Vaquero , Raul D Bertero . *ACI Structural Journal* Nov. 2020. 117 (6) p. 81.
- [Ali and White (2001)] ‘Automatic Generation of Truss Model for Optimal Design of Reinforced Concrete Structures’. M A Ali , R N White . *ACI Structural Journal* July-Aug. 2001. 98 (4) p. .
- [Shobeiri and Ahmadi-Nedushan ()] ‘Bi-directional evolutionary structural optimization for strut-and-tie modelling of three-dimensional structural concrete’. V Shobeiri , B Ahmadi-Nedushan . *Engineering Optimization* 2017. 49 (12) p. .
- [Almeida et al. ()] ‘Comparative analysis of strut-and-tie models using Smooth Evolutionary Structural Optimization’. V S Almeida , H L Simonetti , L O Neto . *Engineering Structures* 2013. 56 p. .
- [Bogomolny and Amir ()] ‘Conceptual design of reinforced concrete structures using topology V. Conclusions © 2023 Global Journals optimization with elastoplastic material modeling’. M Bogomolny , O Amir . *Int. J. Numer. Meth. Engng* 2012. 90 p. .
- [Dunning et al. ()] ‘Coupled aerostructural topology optimization using a level set method for 3D aircraft wings’. P D Dunning , B K Stanford , H A Kim . *Struct Multidisc Optim* 2014. 51 (5) p. .
- [Schlaich and Schäfer ()] ‘Design and detailing of structural concrete using strut-and-tie models’. J Schlaich , K Schäfer . *Struct Eng* 1991. 69 (6) p. .
- [Design of Concrete Structures for Buildings ()] *Design of Concrete Structures for Buildings*, 1984. Toronto, ON, Canada: Canadian Standards Association (CSA). CSA. (CAN3-A23.3-M84)
- [Muttoni et al. ()] *Design of Concrete Structures with Stress Fields, 1st ed*, A Muttoni , J Schwartz , B Thürlimann . 1996. Basel: Birkhäuser Verlag.
- [Kwak and Noh ()] ‘Determination of strut-and-tie models using evolutionary structural optimization’. H G Kwak , S H Noh . *Engineering Structures* 2006. 28 (10) p. .
- [Deutsche Norm, Concrete, Reinforced and Prestressed Concrete Structures-Part 1:3 Design and Construction, Corrigenda to DIN] *Deutsche Norm, Concrete, Reinforced and Prestressed Concrete Structures-Part 1:3 Design and Construction, Corrigenda to DIN*, 1045-1:2001- 07.
- [different material properties in tension and compression Struct Multidisc Optim ()] ‘different material properties in tension and compression’. 10.1007/s00158-011-0633-z. <https://doi.org/10.1007/s00158-011-0633-z> *Struct Multidisc Optim* 2011. 44 p. .
- [Tuchscherer et al. ()] ‘Evaluation of existing strut-And-tie methods and recommended improvements’. Robin G Tuchscherer , David B Bircher , Christopher S Williams , Dean J Deschenes , Oguzhan Bayrak . *ACI structural journal* 2014. 111 (6) p. .
- [Chen et al. ()] ‘Evaluation of strut-and-tie model applied to deep beam with opening’. B S Chen , M J Hagenberger , J E Breen . *ACI Structural Journal* 2002. 99 (2) p. .
- [Chen et al. ()] ‘Evaluation of Strut-and-Tie Modeling Applied to Dapped Beam with Opening’. B S Chen , M J Hagenberger , J E Breen . *ACI Structural Journal* 2002. 99 p. .

- 400 [Huang et al. ()] 'Evolutionary topological optimization of vibrating continuum structures for natural frequen-
401 cies'. X Huang , Z H Zuo , Y M Xie . *Computer Structure* 2010. 88 (5-6) p. .
- 402 [Maxwell and Breen ()] 'Experimental Evaluation of Strut-and-Tie Model Applied to Deep Beam with Opening'.
403 B S Maxwell , J E Breen . *ACI Structural Journal* 2000. 97 p. .
- 404 [Liang et al. ()] 'Generating Optimal Strut-and-Tie Models in Prestressed Concrete Beams by Performance-
405 Based Optimization'. Q Q Liang , Y M Xie , G P Steven . *ACI Structural Journal* 2001. 98 (2) p. .
- 406 [Bruggi ()] 'Generating strut-and-tie patterns for reinforced concrete structures using topology optimization'. M
407 Bruggi . *Computers and Structures* 2009. 87 p. .
- 408 [Victoria et al.] *Generation of strut-and-tie models by topology design using*, M Victoria , O M Querin , P Martí
409 .
- 410 [Coelho and Rodrigues ()] 'Hierarchical topology optimization addressing material design constraints and appli-
411 cation to sandwich-type structures'. P G Coelho , H C Rodrigues . *Struct Multidiscip Optim* 2015. 52 (1) p.
412 .
- 413 [Van Dijk et al. ()] 'Level-set methods for structural topology optimization: a review'. N P Van Dijk , K Maute
414 , M Langelaar , F Van Keulen . *Struct Multidiscip Optim* 2013. 48 p. .
- 415 [Wang and Kang ()] *MATLAB implementations of velocity field level set method for topology optimization: an*
416 *80-line code for 2D and a 100-line code for 3D problems. Structural and Multidisciplinary Optimization*, Y
417 Wang , Z Kang . 2021. 64 p. .
- 418 [Svanberg ()] 'Method of moving asymptotes -a new method for structural optimization'. K Svanberg . *Int. J.*
419 *Num. Meth. Eng* 1987. 24 p. .
- 420 [Marti ()] *On plastic analysis of reinforced concrete. Institute of Structural Engineers*, P Marti . 1980. 104.
- 421 [Xia et al. ()] 'Optimization-based three-dimensional strut-and-tie model generation for reinforced concrete'. Yi
422 Xia , ; Matthijs Langelaar , ; Max , A N Hendriks . *Computer-Aided Civil and Infrastructure Engineering*
423 2021. 36 p. .
- 424 [Liang et al. ()] 'Performance-Based Optimization for Strut-Tie Modeling of Structural Concrete'. Q Q Liang ,
425 B Uy , G P Steven . *Journal of Structural Engineering* 2002. 128 (5) p. .
- 426 [Recent Approaches to Shear Design of Structural Concrete Journal of Structural Engineering (1998)] 'Recent
427 Approaches to Shear Design of Structural Concrete'. ASCE-ACI Committee 445. *Journal of Structural*
428 *Engineering* Dec. 1998. 124 (12) p. .
- 429 [Simonetti et al.] 'Reliability-Based Topology Optimization: An Extension of the SESO and SERA Methods
430 for Three-Dimensional Structures'. H L Simonetti , V S Almeida , F De Assis Das Neves , V Del Duca
431 Almeida , L De Oliveira Neto . 10.3390/app12094220.©2023GlobalJournals. [https://doi.org/10.3390/
432 app12094220](https://doi.org/10.3390/app12094220).©2023GlobalJournals *Appl. Sci.* 2022 12 p. 4220.
- 433 [Geevar and Menon ()] 'Strength of Reinforced Concrete Pier Caps-Experimental Validation of Strut-and-Tie
434 Method'. Indu Geevar , ; Devdas Menon . *ACI Structural Journal* 2019. 116 (1) p. .
- 435 [Schlaich and Anagnostou ()] 'Stress fields for nodes of strut-and-tie models'. M Schlaich , G Anagnostou . *Struct*
436 *Eng* 1990. 116 (1) p. .
- 437 [Sethian and Wiegmann ()] 'Structural boundary design via level set and immersed interface methods'. J
438 A Sethian , A Wiegmann . 10.1006/jcph.2000.6581. <http://dx.doi.org/10.1006/jcph.2000.6581>
439 *Journal of Computational Physics* 2000. 163 p. .
- 440 [Kong and Sharp ()] 'Structural idealization for deep beams with web openings'. F K Kong , G R Sharp .
441 *Magazine Concrete Res* 1977. 29 p. .
- 442 [Allaire et al. ()] 'Structural optimization by the level-set method'. G Allaire , F Jouve , A-M Toader . *Free*
443 *boundary problems*, P Colli , C Verdi , A Visintin (eds.) 2003. Birkhäuser Basel. p. .
- 444 [Allaire et al. ()] 'Structural optimization using sensitivity analysis and a level-set method'. G Allaire , F Jouve
445 , A M Toader . *J Comput Phys* 2004. 194 (1) p. .
- 446 [Leu et al. ()] 'Strut-and-tie design methodology for threedimensional reinforced concrete structures'. L J Leu ,
447 C W Huang , C S Chen , Y P Liao . *Journal of structural Engineering* 2006. New York. 132 (6) p. 929.
- 448 [Strömberg ()] 'Topology optimization of structures with manufacturing and unilateral contact constraints by
449 minimizing an adjustable compliance-volume product'. N Strömberg . *Struct Multidiscip Optim* 2010. 42 (3)
450 p. .
- 451 [Liang et al. ()] 'Topology Optimization of Strut-and-Tie Models in Reinforced Concrete Structures Using an
452 Evolutionary Procedure'. Q Q Liang , Y M Xie , G P Steven . *ACI Structural Journal* 2000. 97 (2) p. .
- 453 [Schlaich et al. (1987)] 'Toward a consistent design of structural concrete'. J Schlaich , K Schafer , M Jennewein
454 . *PCI-Journal* May/June, 1987. 32 (3) p. .
- 455 [Marti ()] 'Truss models in detailing'. P Marti . *Concr. Int* 1985. 7 (12) p. .
- 456 [Wang et al. ()] 'Velocity field level-set method for topological shape optimization using freely distributed design
457 variables'. Y Wang , Z Kang , P Liu . *Int J Numer Methods Eng* 2019. 120 p. .